Int Ophthalmol (2019) 39:1533–1542
https://doi.org/10.1007/s10792-018-0966-3

ORIGINAL PAPER

Demonstration of anatomical development of the human macula within the first 5 years of life using handheld OCT

Talal Alabduljalil · Carol A. Westall · Arun Reginald · Sina Farsiu · Stephanie J. Chiu · Alec Arshavsky · Cynthia A. Toth · Wai-Ching Lam

Received: 13 January 2018 / Accepted: 16 June 2018 / Published online: 23 June 2018

Abstract

Purpose To demonstrate the anatomical development of the human macula using handheld spectral domain optical coherence tomography (SD-OCT) during the first 5 years of life.

Methods This study is a cross-sectional, observational case series. Thirty-five normal eyes of 35 full-term/late preterm infants and children under 5 years of age were included. Handheld SD-OCT was used to image the macula of each eye. The data were analyzed using the Duke OCT Retinal Analysis Program v17 software. Retinal thickness maps were generated for the total retinal thickness (TRT), the inner retinal layers thickness (IRL), and the photoreceptor layer thickness (PRL). Based on the early treatment diabetic retinopathy study macular map, average thickness measurements were taken at 4 circles centered on the fovea (diameter): the foveal center (0.5 mm), sector 1 (S1) (1 mm), sector 2 (S2) (3 mm), sector 3 (S3) (6 mm).

Results The median age at participation was 24 months (range 5–52 months). The TRT increased throughout the first 5 years of life, and this increase was statistically significant at the foveal center and S1 ($p = 0.01$, $p = 0.016$, respectively). The IRL did not show any significant change in thickness from birth and throughout the first 5 years of life. The PRL thickness showed thickening in the first 24 months of age at the foveal center and S1 which was statistically significant at S1 ($p = 0.066$, $p = 0.016$, respectively). Interestingly, this PRL thickness increase plateaus beyond 24 months of age. The photoreceptors inner segment/outer segment (IS/OS) band was identified as a distinct layer in all our subjects.

Conclusion Our findings conform with the literature that the anatomical development of the macular IRL completes before 5 months of age and hence before the PRL. We also identify 24 months of age as an important developmental milestone for photoreceptors development in the human macula.

Keywords Human macula · Macular development · Handheld OCT · Bioptigen OCT · Photoreceptor development

T. Alabduljalil (✉) · C. A. Westall · A. Reginald · W.-C. Lam
SickKids Hospital, Department of Ophthalmology and Vision Sciences, University of Toronto, Toronto, Canada
e-mail: dr_talal@me.com

S. Farsiu · S. J. Chiu · A. Arshavsky · C. A. Toth
Vision and Image Processing (VIP) Laboratory, Departments of Ophthalmology and Biomedical Engineering, Duke University, Durham, NC, USA

Introduction

Most of the morphological development of the human macula occurs in the first 5 years of life [1, 2]. The

developmental model for human macula has been well described in vitro using histological specimens [1–3]. The invention of the handheld spectral domain optical coherence tomography (SD-OCT) allowed scientists to study macular morphology in full-term and premature infants in vivo [3–10]. The widespread use of handheld SD-OCT in children to characterize various pediatric macular conditions coupled with the lack of normative data has created a knowledge gap in the literature. Hence, more normative data studies for the different pediatric age groups are needed. In the literature, macular thickness normative data has been published for children 3 years and older [11–15]. However, to date, these data are limited for full-term born children under 5 years of age [8, 10, 16].

The development of the human macula starts in the fetal life. In utero, the fovea can be histologically identified at 11 weeks of gestation [17, 18], while the foveal pit first appears at 24–27 weeks of gestation [1, 3]. At birth, the human fovea has one or two layers of ganglion cells, most of the inner nuclear layer, and a single layer of large cone photoreceptors [1, 3, 18]. The centrifugal displacement of the inner retinal layers continues until 11–15 months of age [2, 10]. At the same time, centripetal migration of cone photoreceptors reaches 50% of adult peak cone density at 45 months of age [2, 10]. The fovea exhibits adult morphology at 13 years of age [3].

Recently the presence of intra-retinal and sub-retinal fluid in premature as well as full-term infants on OCT was identified [4, 7, 9, 19–21]. Longitudinal follow-up studies for similar infants may shed the light on the significance of this finding. Understanding normal anatomical macular development will help in understanding the future impact of this and other macular pathologies in infants and children.

Spaide and Curcio [22] correlated a hyper-reflective OCT band in the outer retina to the ellipsoid zone of the photoreceptor inner segment, also known as inner segment/outer segment (IS/OS) band. In many retinal diseases and retinal degenerations, the preservation of the IS/OS band on OCT has been regarded as a good prognostic factor for visual acuity [23–25]. On correlating OCT reflective bands with histology, the foveal IS/OS band was first detected as thickening of the hyper-reflective retinal pigment epithelium (RPE) band at 40–42 weeks post-menstrual age (PMA) [3, 8]. It was postulated that sometime between full-term birth and 23 months of age, the IS/OS band becomes a distinct hyper-reflective layer [8].

In this cross-sectional case series, we measured the human macular thickness change in vivo during the first 5 years of life using handheld SD-OCT for full-term/late preterm born children. We examined the central 6-mm-diameter macular area. At the same time, we looked at the presence of sub-retinal fluid and a distinctive IS/OS band in our cohort.

Methods

This observational case series was conducted in compliance with the Hospital of SickKids research ethics board. Infants (born between 36 and 40 weeks gestation) and children under 5 years of age undergoing an ocular procedure in the operating room, with at least one normal eye, were selected. After obtaining an informed consent, the normal eye underwent dilated fundus examination and handheld SD-OCT (Bioptigen Inc.) imaging. Thirty-five healthy eyes of 35 children less than 5 years of age were enrolled. Participants were divided into 3 groups by age: group 1 (birth to 12 months old; $n = 5$), group 2 (13–24 months old; $n = 13$), and group 3 (25–60 months old; $n = 17$) (Table 1). Eyes were excluded if there was history of amblyopia, retinal pathology, hazy media, high refractive error (more than 8 diopters), family history of retinal dystrophy, or developmental delay.

OCT imaging session

OCT scans were performed after induction of general anesthesia and before the intended ocular procedure. After dilating the pupils, with the child lying in the supine position, an indirect fundus examination was performed with a 20D lens to confirm a normal fundus examination. To reduce the risk of prolonging anesthesia, only children classified as American Society of Anesthesia class P1 were imaged [26]. A rectangular OCT volume scan was obtained for all subjects. OCT scan parameters were adopted from Maldonado et al. [27], who postulated infants OCT scan parameters that are adjusted for age and age-derived axial length to increase the accuracy and reliability and reduce acquisition time (Table 2).

Table 1 Demographics of study participants (n = 35)

Group	Age (months)	Sex	Diagnosis	Gestational age	Birth weight	
					Lb	Ounces
1	5	F	Congenital cataract*	40	7	3
1	5	M	Retinoblastoma*	40	7	0
1	6	M	Ptosis**	42	8	13
1	7	F	Retinoblastoma*	42	7	2
1	8	M	Iris cyst*	40	7	0
2	14	F	Infantile ET***	37	5	10
2	15	F	Infantile ET***	36	7	0
2	16	F	Infantile ET***	38	6	5
2	16	M	Infantile ET***	39	10	4
2	16	F	PFV*	38	8	6
2	17	M	PFV*	36	6	0
2	18	F	Infantile ET***	40	7	9
2	19	M	Infantile ET***	36	8	0
2	19	M	NLDO**	39	7	8
2	21	M	Infantile ET***	39	7	5
2	22	F	Retinoblastoma*	38	8	0
2	22	F	NLDO**	40	7	10
2	24	M	Iris atrophy*	40	5	14
3	25	M	PFV*	38	8	2
3	26	M	Retinoblastoma*	36	7	11
3	29	F	NLDO**	37	6	3
3	30	M	PFV*	39	8	9
3	33	F	NLDO**	36	5	10
3	34	M	NLDO**	39	8	2
3	34	M	PFV*	37	7	5
3	36	M	Cataract*	40	9	1
3	36	F	Cataract*	40	6	9
3	40	F	Infantile ET***	38		Unknown
3	42	M	Infantile ET***	36	6	5
3	43	M	EUA**	43	8	13
3	46	F	EUA**	40	7	13
3	48	F	Accommodative ET***	36	4	9
3	48	F	Retinoblastoma*	40	7	0
3	48	M	NLDO**	39	6	13
3	52	F	Cataract*	39	5	13

Group 1: birth to 12 months old

Group 2: 13–24 months old

Group 3: 25–60 months old

ET esotropia, *EUA* examination under anesthesia, *NLDO* nasolacrimal duct obstruction, *PFV* persistent fetal vasculature

*The affected eye was excluded, the other eye enrolled

**Both eyes were normal, one eye enrolled

***The amblyopic eye was excluded, the other eye enrolled

Segmentation and thickness calculation

The data were analyzed using the Duke OCT Retinal Analysis Program (DOCTRAP) v17 software based on MATLAB (MathWorks, Natick, MA). Segmentation was performed semiautomatically in two steps. First, retinal layer boundaries were automatically identified using the technique described previously [28]. In the second step, all segmented retinal boundaries were carefully monitored by a manual grader and the boundary lines were adjusted by the grader utilizing DOCTRAP's graphical user interface. The retinal thickness analyses were performed for the following retinal layers: the inner retinal layer (IRL) extending from the inner aspect of the internal limiting membrane (ILM) to the outer boundary of the outer

Table 2 OCT parameters in different age groups

OCT parameters	Group 1	Group 2	Group 3
Reference arm length (microns)	810	790	780
Scan length (mm)	7.8	8.7	8.3
Number of A-scan/B-scan	1140 × 100	1250 × 100	1360 × 100

Group 1: birth to 12 months old

Group 2: 13–24 months old

Group 3: 25–60 months old

plexiform layer (OPL), the photoreceptor layer (PRL) extending from the outer aspect of the outer plexiform layer to the inner surface of the RPE, and the total retinal thickness (TRT) enclosing all retinal tissue from the inner surface of the ILM to the inner surface of the RPE.

Primary outcome measure

Using the early treatment diabetic retinopathy study (ETDRS) macular grid, the TRT, IRL, PRL average area thickness was computed at the foveal center (0.5 mm), sector 1 (S1; 1 mm), sector 2 (S2; 3 mm), and sector 3 (S3; 6 mm) diameter circles centered on the fovea.

Statistical data analysis

The characteristics of the participating children were analyzed with appropriate descriptive statistics, using means with standard deviations for the normally distributed continuous data. The age was plotted against the IRL, PRL, and TRT thickness to visualize the trend of retina thickness change as age increase.

Formal analysis was performed using the generalized equation estimation (GEE) approach to fit the linear regression on repeated measurements. Correlations among the four sectors (foveal center, S1, S2, and S3) were accounted for by specifying the correlation matrix. Initially, a univariate analysis was used to test the degree of association between the covariates (age and group) and the outcome (IRL, PRL, TRT).

Since only two covariates were of interest, we put both of them in the multiple regression model to test the effect of the covariates. The unstructured correlation matrix was chosen based on the fact that there were four sectors in this study. The final model was chosen based on the interest of covariates and lowest Akaike information criterion (AIC). (The AIC is a measure of the quality of a statistical model relative to other models.) For the photoreceptor thickness, the linear regression model was fitted separately before and after 24 months of age. Predicted plots were plotted to graphically show the final model.

SAS version 9.3 and PROC mixed with repeated statement were mainly used during all the analyses.

Results

Thirty-five normal eyes of 35 participants were analyzed (Table 1). The median gestational age at birth was 39 weeks (range 36–43 weeks; SD 1.85 weeks). The median age at participation was 24 months (range 5–52 months; SD 13.6 months). Among the participants, there were 18 males and 17 females. The mean retinal layer thickness, range, and standard deviation are provided for each age group in Table 3. An age-adjusted macular grid with normal TRT values is illustrated in Fig. 1.

Foveal center and sector 1

The mean TRT in the foveal center: group 1 = 163 microns (range 153–181 microns; SD 11 microns), group 2 = 174 microns (range 146–210 microns; SD 17 microns), and group 3 = 190 microns (range 151–244; SD 24 microns). Our analysis showed that the TRT continues to steadily increase in thickness throughout the first five years of life in these two regions (Fig. 2). Based on our statistical model, the TRT thickness increase with age was statistically significant at the foveal center ($p = 0.01$) and sector 1 ($p = 0.016$).

Table 3 Retinal thickness and segmentation

Macular location	Age group	TRT (microns)			IRL (microns)			PRL (microns)		
		Mean	Range	SD	Mean	Range	SD	Mean	Range	SD
Foveal center	1 (n = 5)	163	153–181	11	51	34–75	15	112	95–137	14
	2 (n = 13)	174	146–210	17	48	26–94	18	127	103–139	10
	3 (n = 17)	190	151–244	24	64	21–160	33	126	84–151	16
Sector 1	1 (n = 5)	204	189–221	13	100	91–123	12	105	96–124	10
	2 (n = 13)	207	189–233	15	84	61–110	15	123	104–136	7
	3 (n = 17)	226	184–276	25	101	53–196	33	125	79–149	15
Sector 2	1 (n = 5)	274	253–298	16	182	156–204	17	93	89–97	3
	2 (n = 13)	291	273–313	10	181	166–204	11	110	99–121	6
	3 (n = 17)	297	276–323	15	184	162–234	17	113	81–134	12
Sector 3	1 (n = 5)	247	230–256	9	156	143–169	9	91	84–98	5
	2 (n = 13)	262	225–318	22	161	134–218	22	101	88–115	7
	3 (n = 17)	259	228–282	16	157	135–203	16	102	77–121	11

Age group 1: birth to 12 months old

Age group 2: 13–24 months old

Age group 3: 25–60 months old

IRL: inner retinal layers (from Inner surface of ILM to outer surface of outer plexiform layer)

PRL: photoreceptors layer (from outer surface of outer plexiform layer to the inner surface of the RPE)

SD: standard deviations from the mean

Foveal center: 0.5 mm diameter centered on the fovea

Sector 1: 1 mm circle centered around the fovea

Sector 2: 3 mm circle centered around the fovea

Sector 3: 6 mm circle centered around the fovea

TRT: total retinal thickness in microns

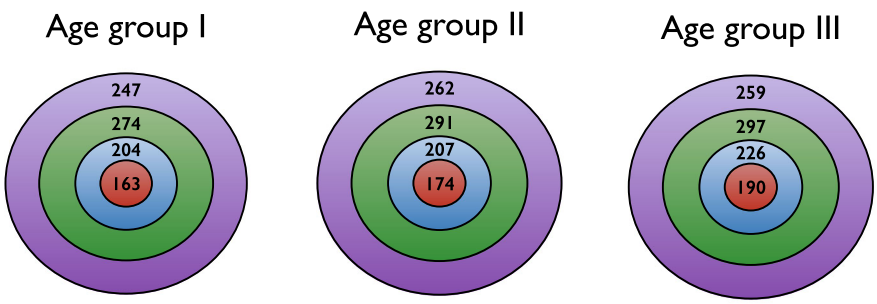

Fig. 1 Average total retinal thickness in microns. Foveal center (central 0.5-mm-diameter centered on the fovea): red. Sector 1 (1-mm-diameter circle centered on the fovea): blue. Sector 2 (3–mm-diameter circle centered on the fovea): green. Sector 3 (6-mm-diameter circle centered on the fovea): purple. Age group 1: birth to 12 months old. Age group 2: 13–24 months old. Age group 3: 25–60 months old

The IRL at the foveal center and at S1 did not change in group 2 compared to the younger group 1. The statistical analysis for IRL trend change over the first 5 years of life at the foveal center and S1 did not show significance (p = 0.097) and (p = 0.24), respectively (Fig. 3).

The PRL showed steep thickening in the first 24 months of age at the foveal center and S1

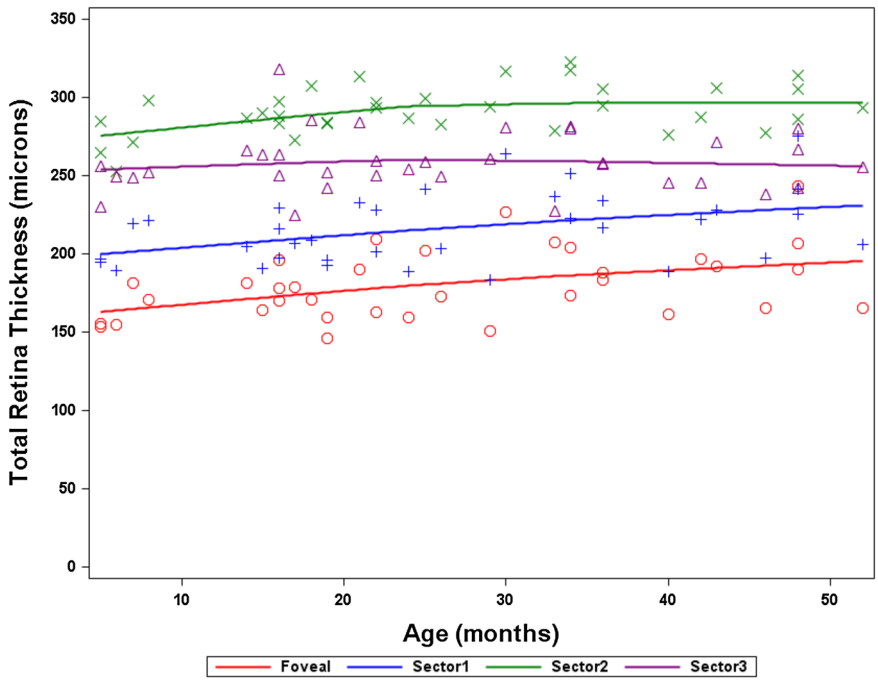

Fig. 2 Total retinal thickness change in microns over the first 5 years of life. The total retinal thickness increases in thickness in the first 5 years of life at the foveal center, sector 1, sector 2 which was statistically significant ($p = 0.01$; $p = 0.016$; $p = 0.017$), respectively. But the change in sector 3 was not statistically significant

($p = 0.031$ and $p = 0.016$, respectively). This is consistent with photoreceptor packing during macular development. Interestingly, we identified that this photoreceptor layer thickening plateaued beyond 24 months of age as shown in Fig. 4.

Sectors 2 and 3

In this region of the macula, the retinal development exhibited minimal thickness change. The TRT continued to steadily increase in thickness throughout the

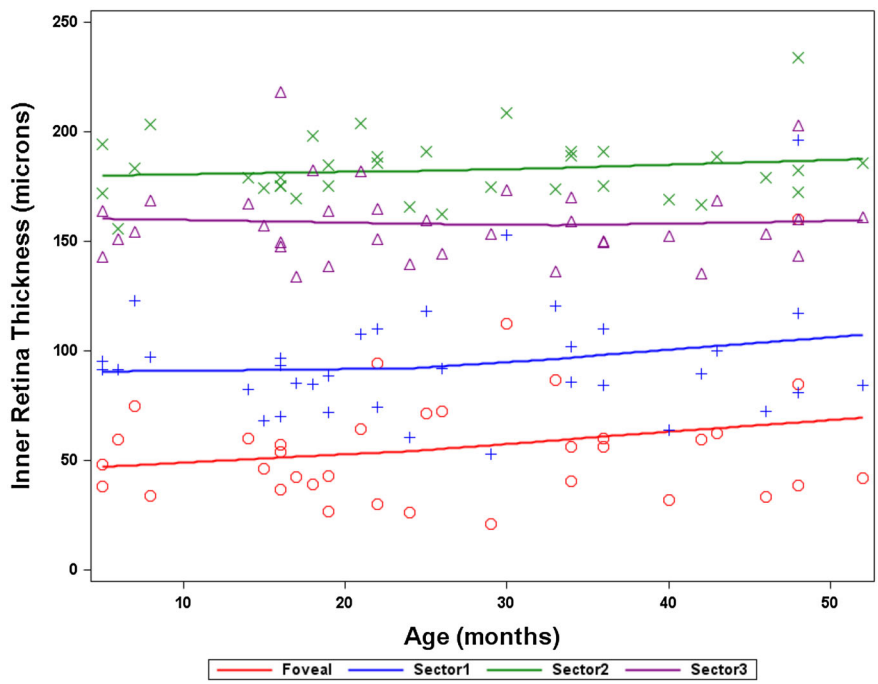

Fig. 3 Inner retina thickness change in microns over the first 5 years of life. The inner retinal layers thickness did not seem to change between term birth and 5 years of life in any sector (see limitations in discussion)

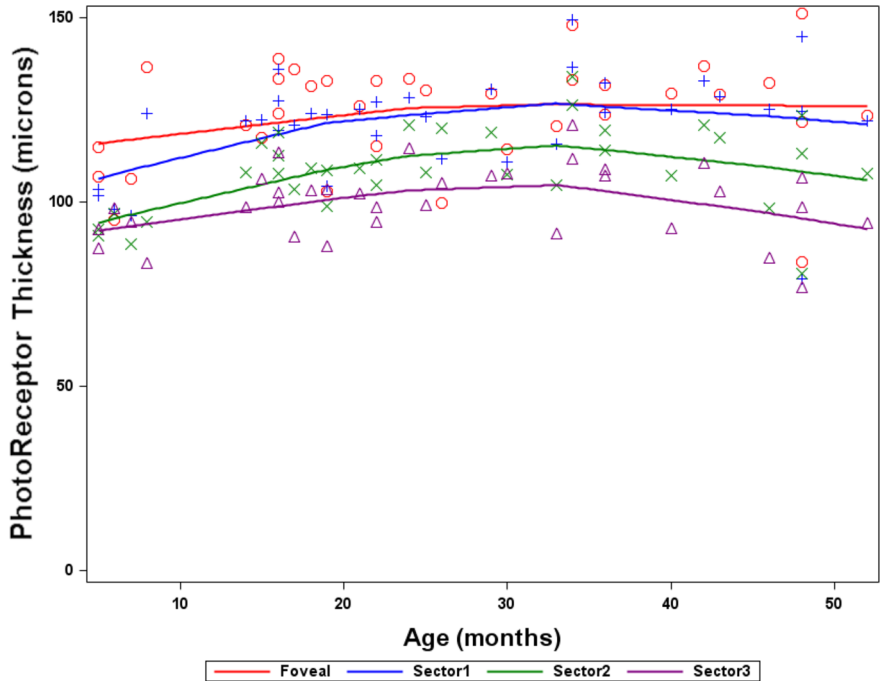

Fig. 4 Photoreceptor layer thickness change in microns over the first 5 years of life. The photoreceptor layer thickness increases steeply over the first 24 months of life then plateaus beyond that. This was seen at the foveal center, sector 1 and sector 2, which was statistically significant ($p = 0.03$; $p = 0.016$; and $p = 0.004$, respectively). This change in thickness was not seen at sector 3

first 5 years of life in S2 ($p = 0.017$). TRT showed no change with age in S3 ($p = 0.79$). The IRL did not show any change in thickness in this region of the macula. At the same time, the PRL showed an increase in thickness in S2 in the first 24 months of life ($p = 0.004$). This change was not seen in S3 ($p = 0.59$). This may indicate that cone packing takes place mostly in the central 3 mm of the macula (foveal center and S1).

Other findings

In our study cohort, no subject had intra-retinal or sub-retinal fluid. The IS/OS band was identified as a distinct hyper-reflective layer in all our study participants in all sectors.

Discussion

In this case series, we were able to demonstrate the retinal thickness change corresponding to the different stages of macular development in humans using the spectral domain handheld OCT.

The development of the inner retinal layers (IRL) in the first 5 years of life

The IRL, as defined in our paper, includes: the nerve fiber layer (NFL), the ganglion cell layer (GCL), the inner plexiform layer (IPL), the inner nuclear layer (INL), and the OPL. In histological studies, the centrifugal displacement of the IRL has been detected in utero at 25-week gestation and was estimated to complete by 11–15 months of age [2, 3, 29]. In our cohort, there was no significant change in the IRL thickness in the foveal center and S1 during the first 2 years of life (Table 1). The IRL centrifugal displacement is best demonstrated if the central foveal thickness is measured as a point and compared to the peri-foveal area [6]. Nevertheless, in the current paper we measured the average of the central 0.5 mm of the fovea as the foveal center and the central 1 mm as S1. In our subjects, both the foveal center and S1 contained IRL, even after the centrifugal displacement of the IRL in age group 3. This accounted for an increase in IRL thickness in the foveal center and S1 in group 3. Maldonado et al. [6] illustrated that much of IRL migration takes place before 42 weeks post-menstrual age (PMA) that is 2 weeks after term birth. Lee et al. [10], on the other hand, have demonstrated that the IRL regression is completed at 17.5 months of

age. In our cohort, the IRL did not change in thickness with age in S2 and S3, suggesting that the centrifugal IRL migration took place within the central 1 mm of the fovea.

The development of the photoreceptors layer in the first 5 years of life

Most of the foveal morphological changes and development after birth took place in the outer retina. The PRL in our paper refers to the outer nuclear layer (ONL), external limiting membrane (ELM), inner segment (IS), EZ, and outer segment (OS). As a result of the overwhelming PRL packing and thickening in the foveal center and S1, and the minimal changes in IRL thickness after birth, the TRT increased steadily during the first 5 years of life. Our study was the first to show a plateau in PRL thickening at 24 months of age in the central 3 mm of the fovea (Fig. 4). Using histological examination and OCT, Dubis et al. [30] indicated that the morphological development of the fovea may be completed by 17 months of age. However, Maldonado et al. [6] showed that the PRL is not of adult thickness at 15 months of age. Some histological studies concluded that the fovea reaches adult morphology between 15 and 45 months [1]. Meanwhile, more recent histological studies identified cone packing to be completed well beyond 45 months of age [2, 3]. Lee et al. [10] have demonstrated that the outer retinal layers reached 99% of its final thickness at 47 months of age and 100% at 75 months of age.

Intra-retinal/sub-retinal fluid

Cabrera et al. [7] described the finding of sub-retinal fluid in 15% and sub-retinal hemorrhage in 21% of their normal full-term cohort. Nevertheless, all of our participants did not have intra-retinal/sub-retinal fluid or sub-retinal hemorrhage. In their case series, Michelle et al. examined all of their participants within 2 days after birth. Beyond 2 months of age, none of their participants had sub-retinal fluid or hemorrhage. In our study cohort, the youngest child was imaged at 5 months of age.

The IS/OS band

The IS/OS band has been regarded as an important surrogate for visual acuity potential. It is essential to understand the timeline and checkpoints for the IS/OS band development. It has been postulated that the IS/OS band is first identified as a thickening of the hyperreflective RPE band at term [3, 8]. However, somewhere between full-term birth and 23 months of age is the proposed period when the IS/OS band is identified as a distinct layer [8]. In our cohort, all participants had a distinct IS/OS band in the foveal center and in all sectors. Vajzovic et al. [16] examined the IS/OS band presence in 47 full-term infants between 37 and 42 weeks PMA. They found out that 47% had an identifiable IS/OS band on handheld SD-OCT. Maldonado et al. [6] studied 4 full-term infants and noted the absence of IS/OS band at 2 months of age, but the IS/OS band was present at 1.5 and 4 months of age, indicating some normal variability in IS/OS band development. The evidence from the literature in combination with our study findings suggests that half of the full-term new born infants will have their IS/OS band at birth and the other half should develop it in the first 5 months of life.

Our study has the limitations of a small, observational, cross-sectional study. Our subject numbers are too small to provide normative data for this age group, specially in group 1 ($n = 5$). However, it is a challenge to image normal infant and children under 1 year in adequate numbers. We did not measure the central foveal thickness point, rather we measured an average of the central 0.5 mm of the foveal. This has limited our ability to demonstrate IRL centrifugal displacement. Furthermore, the production of more studies to examine the foveal development at different time points, in the future, will provide more knowledge to draw the full picture of human macular and foveal development. Many of our participants had ocular conditions like retinoblastoma and congenital esotropia. Despite our best efforts to select the normal, unaffected, non-amblyopic eye, there is very little known on whether such conditions can affect the retinal development of the apparently healthy eye. Another limitation of our study is the measurement of the ONL thickness by using images from a commercial SD-OCT system. Recent studies have shown that some retinal structures including Henle's fiber layer (HFL) exhibit reflectivities that depend on OCT illumination angle [31]. In some significantly tilted B-scans, this phenomenon may affect the accuracy of the ONL measurements from images obtained by conventional OCT systems. Novel OCT systems have

been very recently developed to address this shortcoming in adults [32]. Development and utilization of these novel OCT systems for pediatric subjects are part of our ongoing work.

Conclusion

We demonstrated progressive macular retinal thickening in the first 5 years of life using handheld SD-OCT. There was a steep initial PRL thickening during the first 2 years followed by a plateau. Our findings conform with the literature that the anatomical development of the macular IRL is complete at least before 5 months of age and hence before the PRL. We further propose that 24 months of age are an important developmental milestone for photoreceptors development in the human macula.

Acknowledgements Authors acknowledge the University of Toronto, Ophthalmology research funds committee (ORFC) at the hospital of SickKids for their sponsorship, Cynthia VandenHoven for her help with imaging, Duke University team for the software analysis, and Xiuyan Zhao for the statistical analysis.

References

1. Hendrickson AE, Yuodelis C (1984) The morphological development of the human fovea. Ophthalmology 91(6):603–612
2. Yuodelis C, Hendrickson A (1986) A qualitative and quantitative analysis of the human fovea during development. Vis Res 26(6):847–855
3. Hendrickson A, Possin D, Vajzovic L, Toth CA (2012) Histologic development of the human fovea from midgestation to maturity. Am J Ophthalmol 154(5):767–78 e2
4. Chavala SH, Farsiu S, Maldonado R, Wallace DK, Freedman SF, Toth CA (2009) Insights into advanced retinopathy of prematurity using handheld spectral domain optical coherence tomography imaging. Ophthalmology 116(12):2448–2456
5. Lee AC, Maldonado RS, Sarin N, O'Connell RV, Wallace DK, Freedman SF et al (2011) Macular features from spectral-domain optical coherence tomography as an adjunct to indirect ophthalmoscopy in retinopathy of prematurity. Retina 31(8):1470–1482
6. Maldonado RS, O'Connell RV, Sarin N, Freedman SF, Wallace DK, Cotten CM et al (2011) Dynamics of human foveal development after premature birth. Ophthalmology 118(12):2315–2325
7. Cabrera MT, Maldonado RS, Toth CA, O'Connell RV, Chen BB, Chiu SJ et al (2012) Subfoveal fluid in healthy full-term newborns observed by handheld spectral-domain optical coherence tomography. Am J Ophthalmol 153(1):167–75 e3
8. Vajzovic L, Hendrickson AE, O'Connell RV, Clark LA, Tran-Viet D, Possin D et al (2012) Maturation of the human fovea: correlation of spectral-domain optical coherence tomography findings with histology. Am J Ophthalmol 154(5):779–89 e2
9. Cabrera MT, O'Connell RV, Toth CA, Maldonado RS, Tran-Viet D, Allingham MJ et al (2013) Macular findings in healthy full-term Hispanic newborns observed by hand-held spectral-domain optical coherence tomography. Ophthalmic Surg Lasers Imaging Retin 44(5):448–454
10. Lee H, Purohit R, Patel A, Papageorgiou E, Sheth V, Maconachie G et al (2015) In vivo foveal development using optical coherence tomography. Investig Ophthalmol Vis Sci 56(8):4537–4545
11. Huynh SC, Wang XY, Rochtchina E, Mitchell P (2006) Distribution of macular thickness by optical coherence tomography: findings from a population-based study of 6-year-old children. Investig Ophthalmol Vis Sci 47(6):2351–2357
12. Huynh SC, Wang XY, Burlutsky G, Rochtchina E, Stapleton F, Mitchell P (2008) Retinal and optic disc findings in adolescence: a population-based OCT study. Investig Ophthalmol Vis Sci 49(10):4328–4335
13. El-Dairi MA, Asrani SG, Enyedi LB, Freedman SF (2009) Optical coherence tomography in the eyes of normal children. Arch Ophthalmol 127(1):50–58
14. Eriksson U, Holmstrom G, Alm A, Larsson E (2009) A population-based study of macular thickness in full-term children assessed with Stratus OCT: normative data and repeatability. Acta Ophthalmol 87(7):741–745
15. Yanni SE, Wang J, Chan M, Carroll J, Farsiu S, Leffler JN et al (2012) Foveal avascular zone and foveal pit formation after preterm birth. Br J Ophthalmol 96(7):961–966
16. Vajzovic L, Rothman AL, Tran-Viet D, Cabrera MT, Freedman SF, Toth CA (2015) Delay in retinal photoreceptor development in very preterm compared to term infants. Investig Ophthalmol Vis Sci 56(2):908–913
17. Linberg KA, Fisher SK (1990) A burst of differentiation in the outer posterior retina of the eleven-week human fetus: an ultrastructural study. Vis Neurosci 5(1):43–60
18. Hendrickson A (1992) A morphological comparison of foveal development in man and monkey. Eye (Lond) 6(Pt 2):136–144
19. Vinekar A, Avadhani K, Sivakumar M, Mahendradas P, Kurian M, Braganza S et al (2011) Understanding clinically undetected macular changes in early retinopathy of prematurity on spectral domain optical coherence tomography. Investig Ophthalmol Vis Sci 52(8):5183–5188
20. Maldonado RS, O'Connell R, Ascher SB, Sarin N, Freedman SF, Wallace DK et al (2012) Spectral-domain optical coherence tomographic assessment of severity of cystoid macular edema in retinopathy of prematurity. Arch Ophthalmol 130(5):569–578
21. Dubis AM, Subramaniam CD, Godara P, Carroll J, Costakos DM (2013) Subclinical macular findings in infants screened for retinopathy of prematurity with spectral-domain optical coherence tomography. Ophthalmology 120(8):1665–1671

22. Spaide RF, Curcio CA (2011) Anatomical correlates to the bands seen in the outer retina by optical coherence tomography: literature review and model. Retina 31(8):1609–1619
23. Oishi A, Otani A, Sasahara M, Kojima H, Nakamura H, Kurimoto M et al (2009) Photoreceptor integrity and visual acuity in cystoid macular oedema associated with retinitis pigmentosa. Eye (Lond) 23(6):1411–1416
24. Sallo FB, Peto T, Egan C, Wolf-Schnurrbusch UE, Clemons TE, Gillies MC et al (2012) The IS/OS junction layer in the natural history of type 2 idiopathic macular telangiectasia. Investig Ophthalmol Vis Sci 53(12):7889–7895
25. Testa F, Melillo P, Di Iorio V, Orrico A, Attanasio M, Rossi S et al (2014) Macular function and morphologic features in juvenile Stargardt disease: longitudinal study. Ophthalmology 121(12):2399–2405
26. Kiringoda R, Thurm AE, Hirschtritt ME, Koziol D, Wesley R, Swedo SE et al (2010) Risks of propofol sedation/anesthesia for imaging studies in pediatric research: eight years of experience in a clinical research center. Arch Pediatr Adolesc Med 164(6):554–560
27. Maldonado RS, Izatt JA, Sarin N, Wallace DK, Freedman S, Cotten CM et al (2010) Optimizing hand-held spectral domain optical coherence tomography imaging for neonates, infants, and children. Investig Ophthalmol Vis Sci 51(5):2678–2685
28. Chiu SJ, Li XT, Nicholas P, Toth CA, Izatt JA, Farsiu S (2010) Automatic segmentation of seven retinal layers in SDOCT images congruent with expert manual segmentation. Opt Express 18(18):19413–19428
29. Provis JM, Hendrickson AE (2008) The foveal avascular region of developing human retina. Arch Ophthalmol 126(4):507–511
30. Dubis AM, Costakos DM, Subramaniam CD, Godara P, Wirostko WJ, Carroll J et al (2012) Evaluation of normal human foveal development using optical coherence tomography and histologic examination. Arch Ophthalmol 130(10):1291–1300
31. Lujan BJ, Roorda A, Knighton RW, Carroll J (2011) Revealing Henle's fiber layer using spectral domain optical coherence tomography. Investig Ophthalmol Vis Sci 52(3):1486–1492
32. Carrasco-Zevallos O, Nankivil D, Keller B, Viehland C, Lujan BJ, Izatt JA (2015) Pupil tracking optical coherence tomography for precise control of pupil entry position. Biomed Opt Express 6(9):3405–3419